Chapter 12

Mechanisms of Momentum Transport in Viscous Flow Sintering

Shiva Salem and Amin Salem

Additional information is available at the end of the chapter

http://dx.doi.org/10.5772/53259

1. Introduction

Viscous flow sintering is one of the important processes with a great variety of applications in densification of ceramics. Sintering in the presence of liquid phase makes to fabricate products with low porosity and high technical performance. The most of commercial products such as metals, glass and ceramics with low porosity are fabricated through the viscous flow sintering. The morphology of pores widely affects the characteristics of end product. Adjusting porosity can therefore, control the technical properties of products. During the sintering, the success of process depends on the control of shrinkage and porosity consequently. Many factors affect porosity and characteristics of final product. Some of the most important parameters are the chemical and mineralogical composition of raw materials and mixing ratio of them, glassy phase composition, particle size distribution, temperature and soaking time. Each of these factors can affect shrinkage of product. During the manufacturing process, modification of some parameters may be required to achieve desired porosity. Porosity and pore size distribution of products change with variation in type and content of fluxing materials. Sintering in the presence of liquid phase occurs through the melting flux materials. The molten phase diffuses into the pores by capillary forces, creating closed pores and shrinking the body. The viscosity of molten phase is able to influence shrinkage and porosity of pieces, drastically.

Liquid phase which contains different amounts of oxides greatly affects creeping flow. The mathematically study of momentum transport mechanism can be useful in improvement of microstructure as a result physical-mechanical characteristics of fine ceramics. The term of creeping flow denotes the motion of reactive phase whose Reynolds number is very low. In this chapter the importance of viscous flow in densification and vitrification of ceramics is discussed. The effect of wetting and capillary forces on the motion of liquid phase during

sintering is studied in the other section. Along above dissuasion, the continuity and momentum equations are presented for creeping flow of liquid phase in spherical systems and boundary conditions are considered to obtain velocity distribution. A mathematical model is proposed to describe isothermal variation in porosity of ceramic body according to the observed phenomena. Finally, the kinetics of viscous flow sintering and variations in activation energy and frequency factor are studied. In addition, the computation of optimum sintering time to achieve the minimum porosity at various conditions is explained by kinetic model. The effect of several factors such as amounts of fluxing agents and particle size distribution are verified.

2. Chemical reactions in pre-sintering process

Pre-sintering reactions affect the microstructural development in pieces and consequently, are important in the properties of final products. Firing of ceramics has gained wide recognition in industrial scale, reducing production costs by efficient use of energy in this process. From energy costs point of view, reducing firing temperature or time substantially influences manufacturing costs. There is obviously a maximum heating rate for any ceramic composition that allows thermal reactions to fabricate acceptable properties. Certainly, heating at a slower than maximum rate leads to consider a safe margin for firing process. The firing schedule requires knowledge of chemical reactions and microstructural changes occurring during the process. In this sections a simplified method for determining the optimum firing schedule of ceramics is demonstrated.

The firing profile of a ceramic body may be divided into three parts, representing structural changes that occur with temperature and time [1]. (i) During heating, the green body is a rather fragile and brittle. (ii) After, the formation liquid phase, the viscosity decreases as the maturation temperature rises. In this temperature range that may be called pyroplastic range, which extends into cooling period. Liquid phase loses its viscous characteristics at glass transition temperature. Deformation of body may be occur due to applied stress. (iii) The third division is the final portion of the cooling curve below the glass transition temperature, where the body is a relatively strong and brittle. Thermal shock causing fracture can occur in any of the three divisions but it is most dangerous during heating and cooling when the body is brittle. During the heating, the ceramic body is fragile because of the relatively low inter-particle bond strengths that may be compounded by residual strains from shaping process. During cooling, the ceramic body is relatively strong but is subject to brittle fracture as a result of strain such as phase inversion [2].

In order to design the optimum firing profile, the ideal curve should be determined. The corrections of firing profile can be carried out based on physical and chemical reactions. The actual rate schedule of each of three divisions can be determined. The basic data required can be obtained by simultaneous thermogravimetry and differential scanning calorimetry, TG-DSC or differential thermal analysis, DTA [3,4]. Hot stage microscopy, HSM [5-7], and dilatometeric irreversible and reversible thermal expansion also should be used to optimize heating and cooling stages [1,2].

http://dx.doi.org/10.5772/53259

Figure 1 is an example of TG-DSC curves for a typical porcelain stoneware body for determining physical and chemical reactions in pre-sintering process [8]. These curves show that clay minerals dominate the body in terms of non-linear thermal behavior and the particular temperatures at which the firing profile should be modified. The first and second endothermic peaks around 40–100 ºC in DSC curve is related to the loss of absorbed water. In this temperature range, the absorbed water causes a temperature depression in the body which will increase temperature gradient between the surface and center of pieces. The third endothermic peak, 550 ºC, is due to the dehydroxylation of kaolinite. The weight loss of 2.84 wt.% confirms the elevated percentage of clay minerals. The dehydroxylation of kaolinite occurs to form metakaolin. The crystal structure of kaolinite contains hydroxyl groups and the dehydroxylation of these groups to form metakaolin occurs at 550 ºC. The chemical reaction representing this process is:

$$Al_2O_3.2SiO_2.2H_2O \rightarrow Al_2O_3.2SiO_2 + 2H_2O\uparrow \quad (1)$$

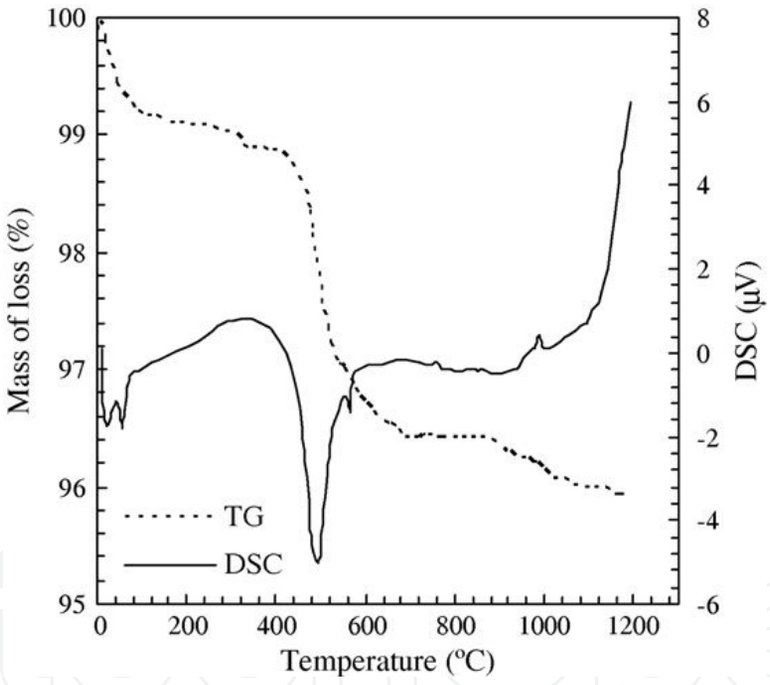

Figure 1. TG-DSC curves of a typical porcelain stoneware composition [8].

Dehydroxylation of clay minerals is observed in typical analytical investigations, such as differential scanning calorimetry and thermogravimetry [9]. These measurements also, are important in the design of fast firing profile. Dehydroxylation rate is directly proportional to the surface area of kaolin. Experiments with large pieces at very high heating rates indicated explosions caused by water vapor pressure at both the dehydration and dehydroxylation temperatures. The last endothermic peak, 571 ºC, is associated with the allotropic transformation of quartz. Because of the relatively great flexibility of the compact particles, the quartz inversion is of little consequence during the firing schedule. The only observed exo-

thermic peak at 988 ºC is typical metakaolin decomposition, forming Al–Si spinel, amorphous silica and mullite phase as shown by following equation:

$$3\left(Al_2O_3.2SiO_2\right) \rightarrow 0.282Al_8\left(Al_{13.33} \oplus_{2.66}\right)O_{32} \quad (2)$$

where ⊕ represents a vacancy. A γ-alumina type phase recently is the predicted product. At 950-1000 ºC, the controversial exothermic peak appears where the excess silica is exolved from the metakaolin to form a precursor for primary mullite crystallization and to begin solid-state and liquid phase. The DSC-TG curves of the body confirm low weight loss, which is mainly due to the metakaolin dehydroxylation. The γ-alumina type phase, being a non-equilibrium unstable phase, certainly transform to mullite above 1000 ºC. The chemical reaction describing the mullite formation is [9]:

$$0.282Al_8\left(Al_{13.33} \oplus_{2.66}\right)O_{32} \rightarrow 3Al_2O_3.2SiO_2 + 4SiO_2 \quad (3)$$

The ceramic bodies generally contain three different mullite that are: (i) Primary mullite from decomposition of pure clay such as kaolinite. (ii) Secondary mullite from reaction of feldspar and clay, clay and quartz. (iii) Tertiary mullite may precipitate from alumina-rich liquid obtained by dissolution of alumina filler [10]. The size and shape of mullite crystals is to large extent controlled by fluidity of the local liquid matrix from which they precipitate, and in which they grow, which itself is a function of its temperature and composition. The composition of this local liquid is determined by the extent mixing of the porcelain raw materials and the role of fluxing agents is critical. The observation of polished and chemically etched surfaces points out as in the samples containing nepheline-syenite, Figure 2. The amount of secondary elongated mullite is larger than in the body prepared without nepheline-syenite. That is essentially due to the lower viscosity of the liquid phase formed in the presence of nepheline, that besides to favor the sintering, allows a better and easy growth of the elongated crystals [11].

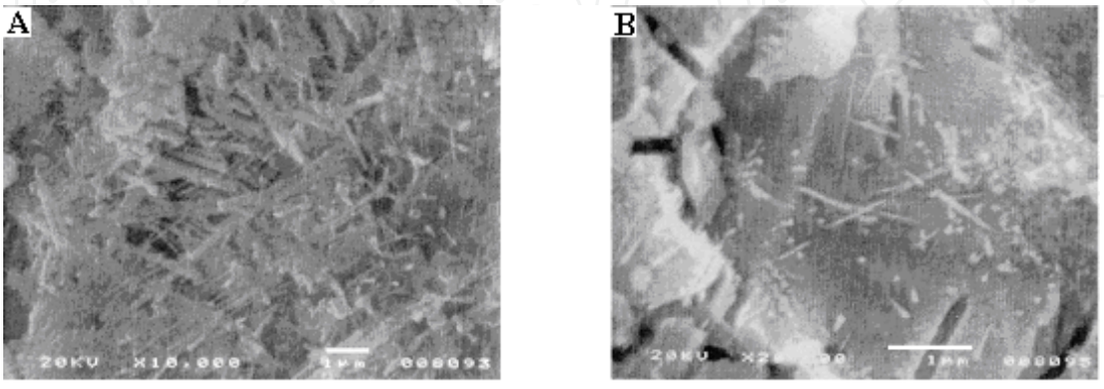

Figure 2. Comparing mullite size in porcelain stoneware body prepared (a) 10 wt.% nepheline syenite and (b) without nepheline syenite [11].

Also, the organic materials burn from 250 ºC onward. The experiments with heavy electrical porcelain result in explosions of body at 250 ºC that is a result of the ignition of volatiles from the lignites in the ball clays.

Hot stage microscopy provides an advantageous data for characterizing the firing and sintering behaviors of ceramic bodies. It allows monitoring of thermal behavior of body from room temperature to sintering steps. The application of this technique to study the sintering of different ceramic substrates was reported by many investigators [5-7]. Hot stage microscopy allows assessing the shrinkage of ceramic body. The compact sample is made from powder by the uniaxial compaction technique. Hot stage microscopy is standard, well-known devices in ceramic and glaze fields. Traditionally, the instrument has found application mainly to assess the thermal behavior, particularly about softening and melting temperatures of glazes, ceramics and other silicate materials. The cylindrical samples of the powders are obtained by pressing in a die at room temperature, usually without addition of any binder. For non-isothermal experiments the furnace of the microscope is heated to the maximum temperature usually with constant rate. The samples are placed on a small ceramic plate with the longitudinal axis coinciding with the vertical direction. By measuring the changes of length and diameter of the samples during the sintering process, either by taking photographs of the sample at pre-chosen time intervals during the sintering process, or by video recording the whole experiment, it is possible to obtain the axial and radial shrinkage. The height and diameter of the photographed or video-recorded sample images can be measured with a relative error, <1%, on suitable enlargement.

To clarify the ability of HSM technique, Figures 3 and 4 show HSM graphs for a typical porcelain stoneware body and a composition modified by 10 wt.% nepheline syenite. Listed below the images is the characteristic shape temperature. Also, the measured valves of reference temperatures for the mentioned compositions are reported in Table 1. The traditional single firing porcelain stoneware composition, reference body, is sintered about 20 ºC higher than sample containing 10 wt.% nepheline syenite. The use of fluxing agent like nepheline syenite in composition clearly shifts the sintering of ceramic body to low temperature because of its tendency to melt and decrease the viscosity of liquid phase. It is evident that the sintering speed of modified composition containing nepheline syenite is enhanced and 20 ºC is enough to obtain well sintered body. The range of dimensional stability is very high for reference composition. When 10 wt.% nepheline-syenite is added, the range of stability drastically reduces, and a negative shrinkage, expansion, is observed. The addition of nepheline causes the decrease in softening temperature.

Nepheline syenite (wt. %)	Starting shrinkage	Maximum Shrinkage	Expansion	Softening point
0.0	1120	1220	1280	1340
10.0	1100	1200	1240	1320

Table 1. The technical temperatures of porcelain stoneware compositions obtained by HSM technique.

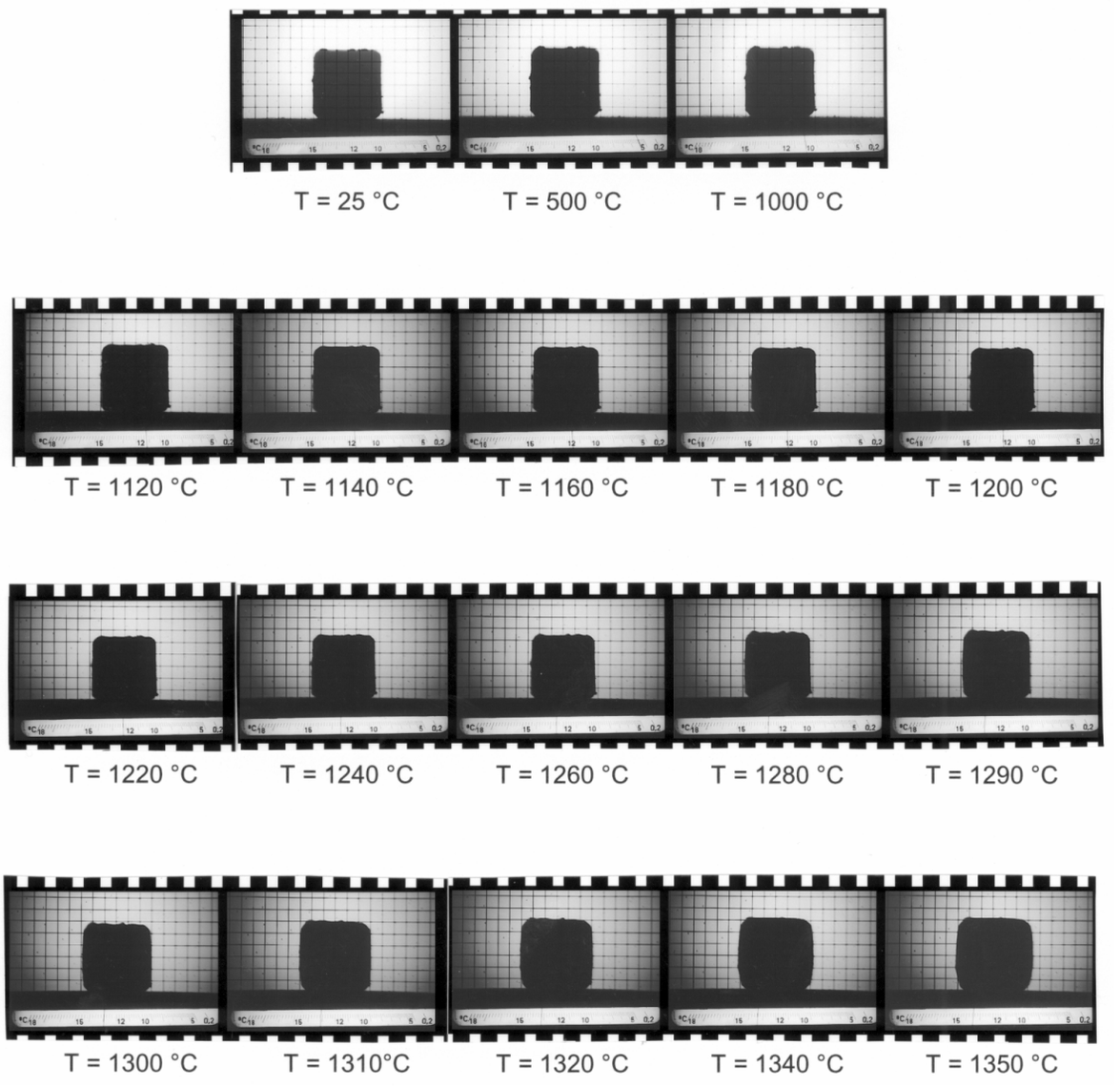

Figure 3. The HSM images of a typical porcelain stoneware composition.

http://dx.doi.org/10.5772/53259

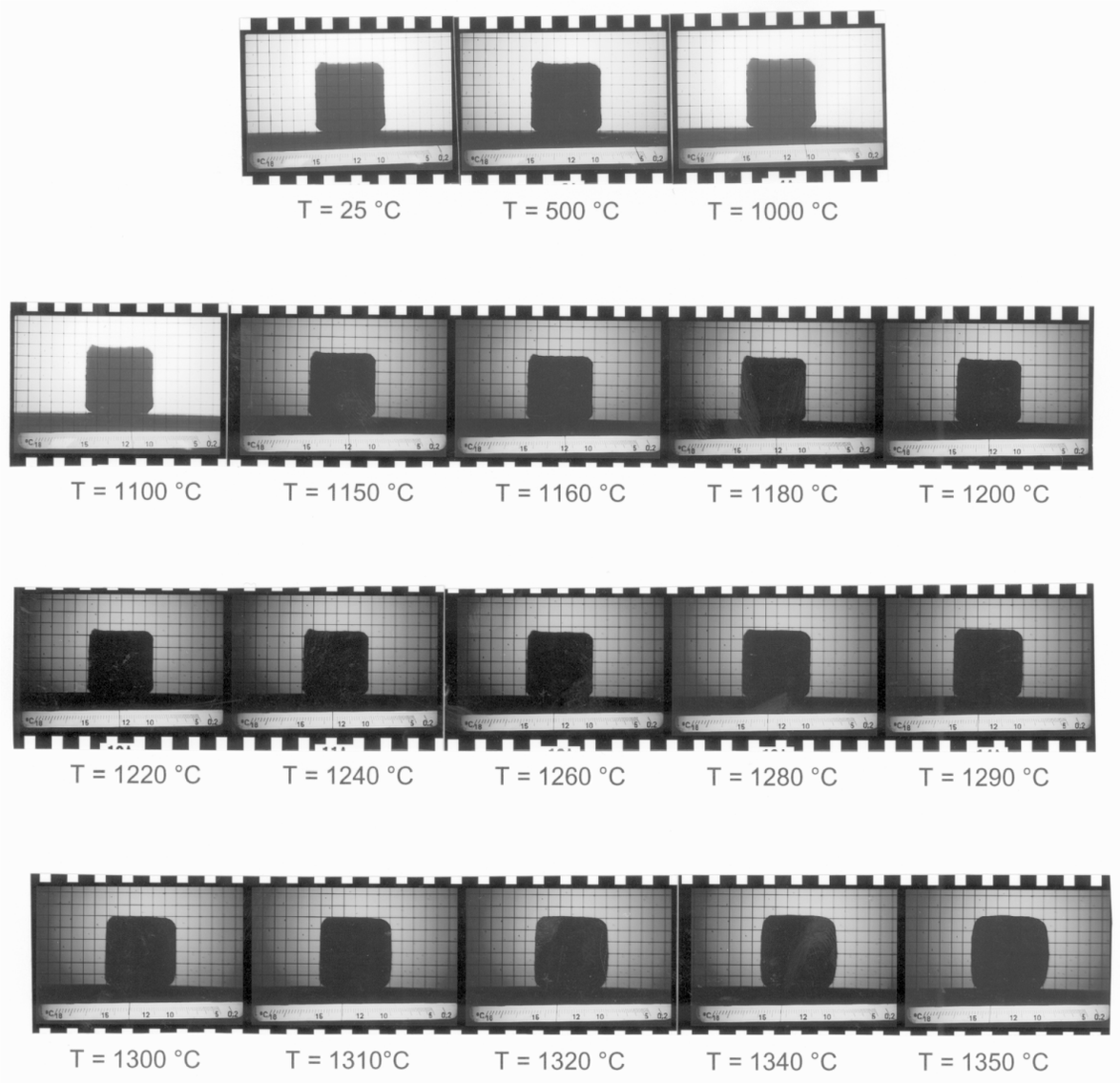

Figure 4. The HSM images of porcelain stoneware composition prepared with 10 wt.% nepheline syenite.

Irreversible thermal expansion curve really consists of behavior of all unfired materials in composition. The thermal expansions of some components are well known. For example, the α-β quartz inversion causes a sharp increase in expansion [9]. Between the 500 and 550 ºC, dehydroxylation of the clay minerals modifies the expansion as the clay is contracted. On the other hand, the fluxing agents like feldspars and nepheline syenite, which undergo no transformations at this temperature range, continue to expand almost linearly. The phenomena around 600 ºC may be quite severe for some clay based ceramics such as porcelains and porcelain stoneware bodies until the dense structure are formed. According the previously explanations, the ceramic body begins to sinter between the 850 to 900 ºC due to expulsion of excess silica released from metakaolin when γ-alumina spinel is crystallized. In this condition the body presents pyoplasticity. When the feldspars begin to melt at 1050 ºC [12,13], the contraction accelerates and pyoplasticity increases remarkably.

The dilatometric curve of a typical porcelain stoneware composition is shown in Figure 5. It is observed that expansion increases until a maximum value about 900 ºC. The sharp increase at 571 ºC is due to α-β quartz inversion. From this temperature onward, the expansion rate gradually decreases and sintering starts at 950 ºC. From 950 ºC, the shrinkage increases in an exponential form with temperature. The shrinkage of ceramic bodies varies with type and content of fluxing materials because, sintering of porcelain bodies occurs through the melting of fluxing materials. The molten phase diffuses into the pores by capillary forces, creating closed pores and shrinking the body. The viscosity of molten phase is able to influence shrinkage and porosity of porcelain stoneware bodies drastically. From dilatometric curves for compositions containing 10 wt.% nepheline syenite, Figure 6, it can be noticed that the shrinkage rate increases. When shrinkage reaches to maximum value at 1225 ºC, the open porosity of body containing nepheline syenite reaches to zero. As a result, the pores of these bodies are closed at this temperature. The use of fluxing agents like nepheline syenite favors the sintering behavior, allowing sintered materials with minimum porosity. The maximum value of shrinkage, reached by the samples containing nepheline is higher than the maximum value of composition prepared without nepheline syenite. Furthermore, it is reached in rather low temperature.

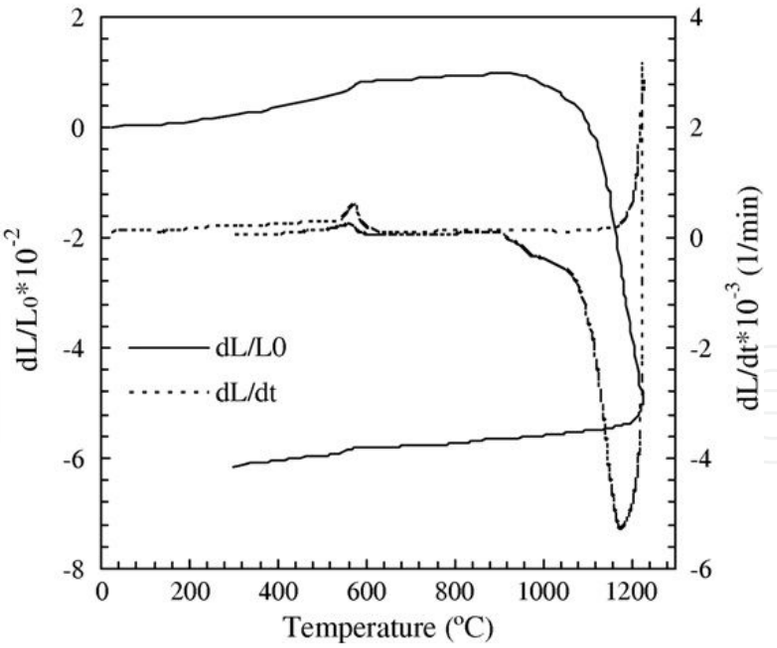

Figure 5. The dilatometeric curves of a typical porcelain stoneware composition.

http://dx.doi.org/10.5772/53259

The reversible thermal expansion occurs in fired ceramics such as electrical porcelain and porcelain stoneware due to the α-β residual quartz inversion at the glass transition temperature in which a viscoelastic material transforms to a elastic solid in cooling stage [2]. The glass content in different porcelains may be vary from 50 to 80 wt.% according the selected composition. Usually porcelain stoneware body shows the inflection at 570-600 ºC but electrical porcelains may not show this inflection clearly due to increasing glass content during firing process. It should be note that the glass phase should be annealed in the cooling to reduce the total stress when the residual quartz inverts at 570-600 ºC. The industrial experiences clearly showed that nothing can prevent the β-α quartz inversion with its consequent stress development in ceramic body. It is interesting to note that quartz particles as small as 1 μm produce crack in porcelain body. Therefore, there are two major sources for development of stress in the cooling of ceramic bodies. If there is no thermal arrest at glass transition temperature, the glass phase will be improperly annealed and strain energy will be stored. When β-α quartz inversion occurs at 570-600 ºC, the inversion stresses are added to the residual glass stresses. If stresses exceed the strength of ceramic body, fracture occurs immediately otherwise, the stresses may be large enough to cause crack growth and it may be developed hours or even months later. Fabricating an absolutely free-stress ceramic body is actually impossible but it is possible to manufacture reliable product by minimizing stress.

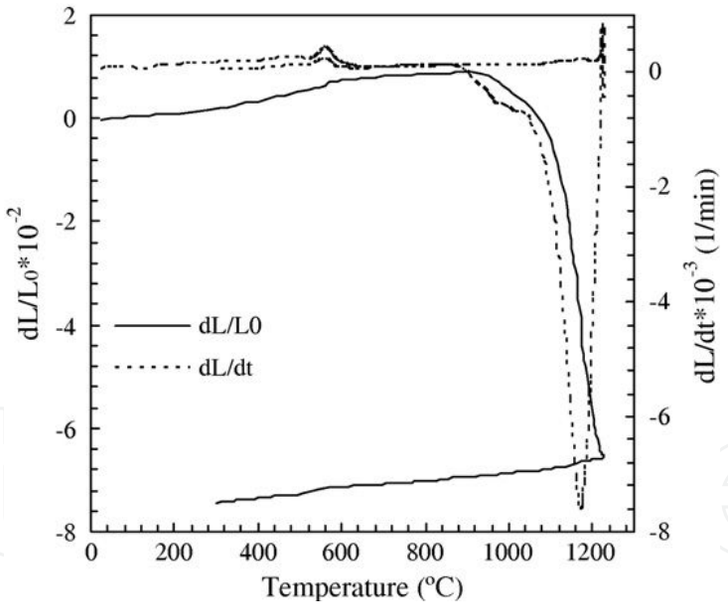

Figure 6. The dilatometeric curves of porcelain stoneware compositions prepared with 10 wt.% nepheline syenite.

In design of firing profile, the irreversible and reversible thermal expansion data should be considered in first step and then it can be modified by DSC or DTA data. This procedure establishes the shape of firing profile at three stages. The heating rate should be separately determined in each section. The irreversible thermal expansion data are used in heating step and the reversible expiation data should be used in design cooling step. Critical points on the profile are identified by DSC or DTA data. Ceramic body can be damaged by steam

pressure at both adsorbed water removal and dehydroxylation of clay occurring in 100 and 550 ºC, respectively. The combustion of volatiles from lignites causes crack in very large cross section bodies. It is important that the ignition of organic materials is completed before the ceramic bodies become impervious. Because the nature of the ceramic bodies are substantially different in the three major section of firing profile, the heating and cooling rates should be determined in next step. The firing profile should be determined empirically if it is not available for a new composition. In summary, the most critical points are between 550 and 600 ºC during the heating. The pyroplastic section may be modified slightly but the maturation should be completed. The cooling profile should be adjusted separately. The ceramic body can almost be quenched from the maturing temperature to 800 ºC and then it should be annealed until 550 ºC by considering the β-*α* quartz inversion.

3. Wetting and liquid migration during sintering

Wetting and surface phenomena play important role in sintering in the presence liquid phase because the surface area of the compact powder reduces during the heating process. Therefore, the microstructure of product is affected remarkably by surface phenomena. The fundamental problem of sintering in the presence liquid phase is explanation of mechanisms that reduction of energy occurs which are especially important for understanding the factors affecting process. During the sintering process the particles weld together and pores between them become more nearly spherical and the porosity of compact decreases simultaneously. The driving force for both phenomena is due to excess surface free energy. An atom at a free surface is bonded to fewer neighboring atoms than an atom within the particles. Since bonding reduces the potential energy, a surface atom has extra energy, called the surface energy, which can be partially reduced by slight adjustments in the composition and bonding between the atoms in the surface. Nevertheless, surface atoms or ions are more active. Thermodynamically, the surface tension, γ, is defined as [1]:

$$\gamma = \left(\frac{\partial G}{\partial A_p} \right)_{P,T,N_i} \tag{4}$$

where, G is the Gibb's free energy of the system. During the change in particle area, A_p, the independent variables of pressure, P, temperature, T, and number of species, N_i, in the system remain constant. If the radius of pore r_1 in ceramic structure is considered as shown in Figure 7, surface tension will tend to contract the surface area and the internal volume, increasing the internal pressure by an increment ΔP. At equilibrium condition, the word of contraction $\Delta P \Delta V$ is equal to the decease in surface free energy γdA.

$$\Delta P 4\pi r_1^2 dr_1 - \gamma 8\pi r_1 dr_1 = 0 \tag{5}$$

http://dx.doi.org/10.5772/53259

Therefore,

$$\Delta P = \frac{2\gamma}{r_1} \tag{6}$$

where ΔP and ΔV are the pressure and volume differences, respectively. In sintering process ΔP are considered respect to atmospheric pressure.

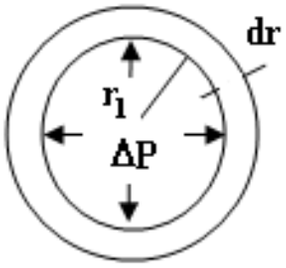

Figure 7. The pressure difference in pore produced by surface tension.

It should be note that the radius r_1 is negative when the curvature is concave. The effect of surface curvature may cause the average chemical potential of atoms in microscopic particles to be greater than that in large particles. The atoms in a microscopic region of sharp positive curvature are of a higher chemical potential than atoms in a flat surface. In this section the interfaces between a solid and liquid phase is considered to study sintering process. Consequently, the surface curvature effect is that equilibrium pressure is a function of surface energy and surface curvature. An example for processing consequence of the surface curvature effect is capillary phenomena. Spreading liquid on solid occurs when the contact angle measured through the liquid phase approaches zero. In the sintering in the presence liquid phase, wetting and spreading phenomena affect the pore morphology as a result microstructure of ceramic body. Liquid phase that wets the surface of particles will spread over the surface and concentrate in contact region, forming necks as shown in Figure 8. The pressure difference across the curved meniscus is negative and a compressive stress occurs in contact region. The pressure differences across a curved meniscus can also, cause the migration of liquid phase between the pores or migration of liquid from a saturated region to a less saturated region.

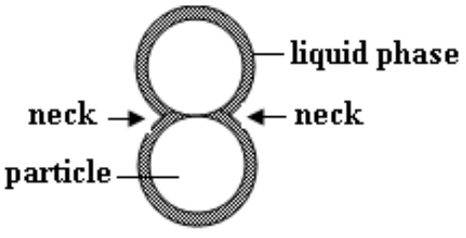

Figure 8. Liquid phase distributed on surface of spherical particles.

As illustrated in Figure 9 liquid phase will rise in capillary spaces if it wets the surface. On the other hand, it will be depressed if non-wetting of particle surface occurs. In this case, it is impossible to sinter the ceramic body. This phenomena rarely observed in sintering ceramic materials. For the fine capillary spaces, the meniscus is approximately hemispherical. At equilibrium condition, this pressure difference will offset the hydrostatic pressure which may rise above the meniscus external to the capillary space. The penetration of liquid into the porous medium will be grater for a liquid lower viscosity and higher surface tension. Finer pores produce a greater suction. An increase in temperature may reduce surface tension/viscosity ratio and improves penetration. In sintering of ceramic bodies in the presence liquid phase, the capillary force provides a mechanism for the cohesion, migration of liquid in pores and rearrangement of particles. Capillary suction produces a driving force for migration of liquid in sintering [14].

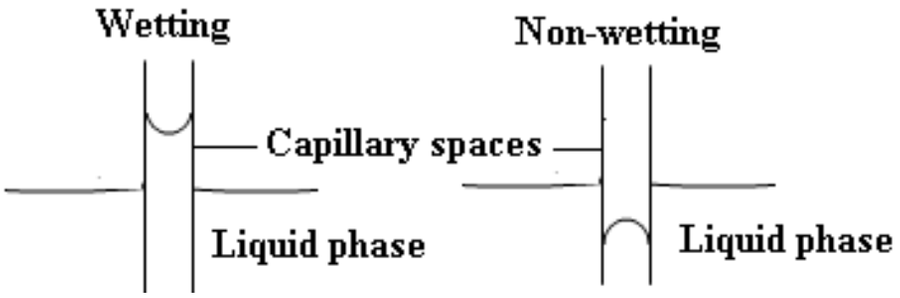

Figure 9. Wetting and non-wetting behaviors of liquid phase.

4. Vitrification and microstructural changes

The vitrification of fine ceramic products such as electrical porcelains, whitewares and porcelain stoneware bodies is complex since sintering occurs with reaction of materials and formation new crystalline and amorphous phases. The glassy phase coats quartz, new crystals such as mullite and cristobalite and remained fluxing agents such as feldspars [9]. The ceramic body shrinks when metakaolin transformed into primary or secondary mullite crystals and amorphous silica between 950 and 1000 ºC. The amorphous silica liberated during the metakaolin decomposition is highly reactive, possibly assisting eutectic melt formation at 990 ºC. Feldspars, minerals with high alkali content, are generally used as fluxing agent in the production of fine ceramics [12]. A eutectic melt of potassium feldspar with silica starts at this temperature. The eutectic temperature depends on the type of feldspar. Sodium feldspar forms eutectic melt at 1050 ºC. The lower liquid formation temperature in potassium feldspar system is beneficial for reducing the ceramic body sintering temperature. The presence of albite in potassium feldspar can reduce the liquid phase formation. Quartz in contact with the feldspar liquid dissolves slowly above 1250 ºC. The rate of mullite formation and quartz dissolving is very dependent on particle size of materials and type of impurities and

secondary fluxing agents. The particular important factors that influence the rate of vitrification are viscosity, surface tension and particle size distribution.

The viscosity of the liquid phase, influenced by the kind of the fluxing agent used and the sintering cycle, is able to drastic affect the microstructure of fired products, in particular to change the amount, morphology and size of the porosity [11]. Nepheline, even if it enters in the formulation of different ceramic products, such as sanitary ware, electrical porcelain and china ware bodies, reduces the firing temperature and increases the alkali level in the glass phase [13]. Nepheline is a major component of several igneous rocks called nepheline-syenite, nepheline-monzonite and nephelinite. The basic difference among these rock types is the amount and type of feldspars present. In nepheline-syenite, feldspars are the most important phase. In the nepheline-monzonite rocks both potassium feldspars and plagioclase are present in nearly equal proportions. In nephelinites there is little feldspar present and the rock is mostly nepheline. Nepheline is a member of the feldspathoid group of silicates, minerals whose chemistry is close to that of the alkali feldspars, but they are poorer in silica. About the use of nepheline and nepheline-syenite for the production of high temperature ceramic products, such as glasses, glass-ceramics or ceramics, it is important to make some distinctions. Nepheline should not be confused with nepheline-syenite, which is actually a mixture of about 55 wt.% albite, 25 wt.% potassium-feldspar and only about 20 wt.% nepheline. The chemical and physical properties are consequently very different. The melting point of pure nepheline is very high, 1520 ºC [13], compared to that of the other feldspars: 1118 ºC for sodium-feldspar, 1150 ºC for potassium-feldspar and, 1223 ºC for nepheline-syenite [12]. Compared to pure feldspars, the advantages coming from the use of nepheline-syenite are: (i) the content of potassium and sodium is higher, K_2O + Na_2O is about 9–12 wt.% in feldspars, whereas it is larger than 14 wt.%, in nepheline syenite, and (ii) the melting temperature is generally lower than that of potassium-feldspar, which always contains other phases, such as quartz, which shift the melting point to higher temperatures. In the glass production, the use of nepheline-syenite provides the necessary additives of alumina and alkali for the glass formulation, and it is low in silica and does not contain free quartz. Furthermore, due to the lower melting point of nepheline-syenite, in comparison with potassium feldspar, the glass batches obtained have lower viscosity and easier workability. The content of Al_2O_3 is high and the content of SiO_2 is lower in nepheline-syenite with respect to feldspars (considering that in feldspar Al_2O_3/ SiO_2 is about 0.2, whereas in nepheline Al_2O_3/SiO_2 is 0.5).

When higher amounts of nepheline-syenite are added, the range of dimensional stability drastically reduces, and a negative shrinkage, expansion, is observed [11]. The fracture surface of a typical porcelain stoneware body is presented in Figure 10(a). It is characterized by the presence of round pores, essentially closed porosity, whose sizes are significantly larger than the ones present in the nepheline-syenite modified composition, Figure 10(b). Spherical pores indicate a mature microstructure, where a sort of equilibrium is reached, from the equilibrium between the pressure of gas and the viscosity of the liquid phase, spherical pore results.

The microstructures of bodies prepared with high amounts of nepheline syenite do not present substantial differences among them [11]. The presence of nepheline-syenite results in fired bodies with a larger degree of vitrification. Even 5 wt.% of nepheline-syenite produces nearly 10 wt.% more glass than the body prepared without nepheline syenite. The glass fraction linearly increases with the amount of nepheline syenite. The crystalline phases, such as quartz and mullite, which are unstable in the alkali oversaturated glass matrix, decompose more easily. The fraction of albite linearly increases with the addition of nepheline-syenite. The replacement of the potassium feldspathic sand with nepheline-syenite strongly favors the sintering behavior of material. Even only a replacement of 5 wt.% of nepheline syenite, causes a drastic decrease of the soaking time necessary to reach a minimum total porosity.

The lower viscosity of the liquid phase, that decreases with the increase of nepheline-syenite, favors the shrinkage, but also the growing of rather large closed pores, that, trapped in the glassy matrix during cooling, cause the observed expansion, for the longer soaking times. The presence of the nepheline-syenite in the body mix strongly favors the sintering behavior to obtain sintered materials with a minimum porosity. The fired modified compositions show homogeneous microstructures, characterized by smaller pores, with a narrow pore size distribution. The use of a 5 wt.% of nepheline-syenite allows reaching the best results. Higher percentages reduce, in an unacceptable way, the range of dimensional stability.

For clay based ceramics the surface tension is not changed much by composition [15,16]. However, surface tension is not a variable that normally causes difficulty during the design of composition or control of sintering process.

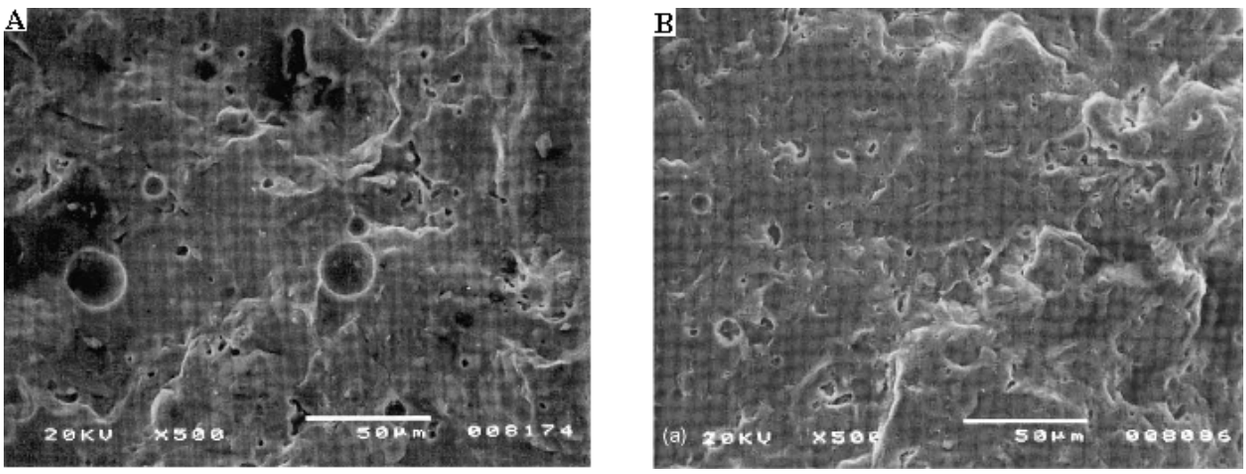

Figure 10. SEM micrograph of the fracture surface of the porcelain stoneware composition prepared (a) without nepheline syenite and (b) 5 wt.% nepheline syenite.

The particle size has a strong effect on the sintering rate and should be controlled if vitrification process is going to be controlled. In changing from 10 to 1 μm particle, the rate of sintering is increases by a factor of 10 [2]. When the porcelain stoneware composition - milled at longer time, the compact microstructure is formed with very few and narrows pores, Figure

http://dx.doi.org/10.5772/53259

11. The increase of the milling time, allowed obtaining a finer powder. As a consequence, more reactive particles are produced, that allows producing a very compact and homogeneous material.

5. Creeping flow

For liquid phase, the physical property that characterizes the resistance to flow is viscosity. Laminar flow is orderly type of flow that is usually observed, in contrast to turbulent flow. In order to characterize the type of fluid flow Reynolds number is used as a follows [17]:

$$N_{Re} = \frac{\varrho u l}{\eta} \tag{7}$$

where N_{Re} is Reynolds number, ϱ is fluid density, u is velocity, l is characteristic length such as diameter and η is viscosity of fluid. Experimental observations show that there are actually three flow regimes and these may be classified according to the Reynolds number for the flow. The three flow regimes are: (i) laminar flow with negligible rippling, $N_{Re}<20$, (ii) laminar flow with pronounced rippling, $20< N_{Re}<1500$, and (iii) turbulent flow with $N_{Re}>1500$. For the Reynolds number less than 20, the ripples are very long. This number is the desired method that provides the flow regime. When is less than 0.1, $N_{Re}<<0.1$, and the flow is carried out slowly, this type of flow is referred as creeping flow or Stokes flow. If the flow of incompressible fluid into the spherical pore is considered, such as viscous flow sintering, the fluid approaches the center of pore diametrically. In this case, the creeping flow means that Reynolds number is less than 0.1.

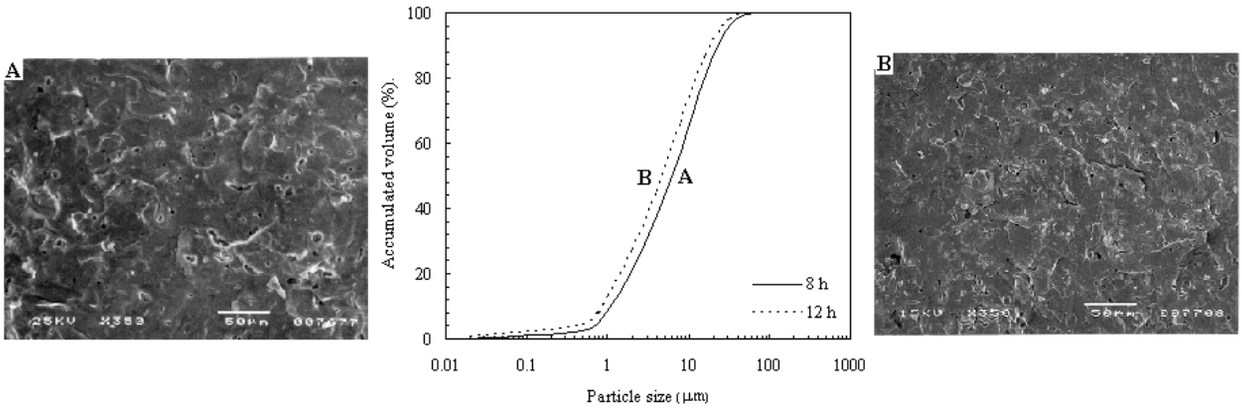

Figure 11. SEM micrograph of the fracture surface of a typical porcelain stoneware composition containing 10 wt.% nepheline syenite milled (a) 8 h (b) 12 h.

6. Continuity and motion equations

In order to calculate the flow characteristics such as average velocity and force, the velocity distribution should be determined by the shell momentum balance method. It is tedious to set up a shell balance for each flow. A general mass and momentum balances that can be applied to each flow are needed, including cases with non-rectilinear motion. These are the main points of this section. The continuity and motion equations that are related to mass and momentum balances respectively, can be used as a starting point for studying the viscous flow. The equation of continuity is developed by making a mass balance over a small element of volume through which the fluid is flowing. Then the desired partial differential equation is generated. The following equation describes the time rate of fluid density at a fixed point in space. This equation can be written more concisely by using vector notation as a follows [17,18]:

$$\frac{\partial \varrho}{\partial t} = -\left(\nabla \varrho u\right) \tag{8}$$

where t is time. This equation shows that the rate of increase of mass per unit volume is equal to net rate of mass addition per unit volume by convection. A very important special form of continuity equation is that for an incompressible fluid. For example, the following particularly simple form is considered in spherical coordinates (r, θ, φ):

$$\frac{1}{r^2}\frac{\partial}{\partial r}\left(r^2 u_r\right) + \frac{1}{r\sin\theta}\frac{\partial}{\partial \theta}\left(u_\theta \sin\theta\right) + \frac{1}{r\sin\theta}\frac{\partial}{\partial \phi}\left(u_\phi\right) = 0 \tag{9}$$

Of course, no fluid is truly incompressible, but the assumption of constant density in viscous flow sintering results in considerable simplification.

The equation of motion is developed by making a momentum balance over a small element of volume and letting the volume element become infinitesimally small. Again a partial differential equation is generated. The equation of motion can be used along with continuity equation to solve many more complicated flow problems. It is a key equation in transport phenomena. The following motion equation was obtained by momentum balance:

$$\frac{\partial}{\partial t}\varrho u = -\left[\nabla.\varrho uu\right] - \nabla.p - \left[\nabla.\tau\right] + f_g \tag{10}$$

where $\nabla.p$ is pressure gradient, $\nabla.\tau$ is divergence of shear stress and f_g is external force acting on fluid per unit volume. For incompressible fluid with Newtonian behavior the motion equation can be written as very famous Navier-Stokes equation. If the acceleration and external force terms in this equation are neglected, the following equation is obtained:

http://dx.doi.org/10.5772/53259

$$\nabla .p=\eta\nabla^2 u \tag{11}$$

which is called the creeping or Stokes flow equation.

7. Velocity distribution in spherical systems

The sintering in the presence of liquid phase is complex process, because a lot of phenomena simultaneously occur during sintering. Raw materials react and new crystalline phases are formed. The melting process of raw material produces a liquid phase whose viscosity decreases by increasing the sintering temperature so that it can enter the pores and eliminate them. Some crystals such as quartz tend to dissolve in the liquid phase. A characteristic shrinkage is observed when the metakaolin formed from the clay minerals at high temperature transforms into needle-shaped mullite crystals in the presence silica glassy phase between 950 and 1000 °C. A liquid phase forms between 950 and 1150 °C when the fluxing agents such as feldspars are presented in contact with silica, eutectic point [1]. The above considerations clearly illustrate that it is impossible to develop a theoretical kinetic model only on the basis of the chemical reactions that occur during sintering. Very few models are developed for the case in which the solid phase partially reacts with the liquid phase but theoretical models are developed by considering the pore size and the shrinkage variations. In those models [19,20] some geometrical assumptions are exaggerated respect to microstructure of compact body. Therefore, the results of these equations have an approximate validity regard to the influence of kinetic parameters such as temperature and soaking time on sintering rate. In the sintering in the presence liquid phase, the viscosity changes continuously by increasing soaking time due to the formation of new crystalline phases and melting of some crystals such as quartz. The average pore size increases progressively and kinetic models were proposed to describe the isothermal sintering based on the average pore size [21-23]. In this section a kinetic model is developed to describe the changes in porosity of compact body during the soaking time, using the Navier-Stokes equation. The sintering process is due to the liquid phase diffusion, by capillary pressure, in the interconnected pores.

The type of pores in compact materials is divided to open and closed pores. An open pore is cavity or channel that communicates with surface of body. Closed pores are located inside of the compact body and are completely isolated from the external surface. The summation of open and closed porosity gives the value of total porosity. The open, total and closed porosity of a special ceramic body versus soaking time are shown in Figure 12. With increasing soaking time both open and total porosity decrease progressively. The closed porosity, however, increases with rising soaking time. The trends of open and total porosity at lower soaking times are very similar, indicating that all pores are open. As the soaking time increases, the value of closed porosity increases, reaching a point where all pores are closed. Scanning electron microscopy observations of fracture surfaces of the bodies show a microstructure which lacks homogeneity, char-

acterized by some closed pores. Longer soaking times favor the development of larger amounts of glassy phase, so the sample becomes more compact and interconnected pores tends to disappear, in agreement with minimum porosity. At the sintering conditions able to reach the minimum porosity, the pores are generally spherical and they are small. It is interesting to note that a too large increase in soaking time causes abnormal growth of the closed pores which in turn, influences mechanical strength. Indeed, the total porosity is affected by two factors. (i) The capillary pressure, due to the surface tension of liquid phase, tends to reduce the pore size, which in turn, reduces the open and total porosity. (ii) The pressure of gas inside the closed pores tends to expand the pores, when the minimum porosity is reached, therefore, the total and closed porosity increase simultaneously [16].

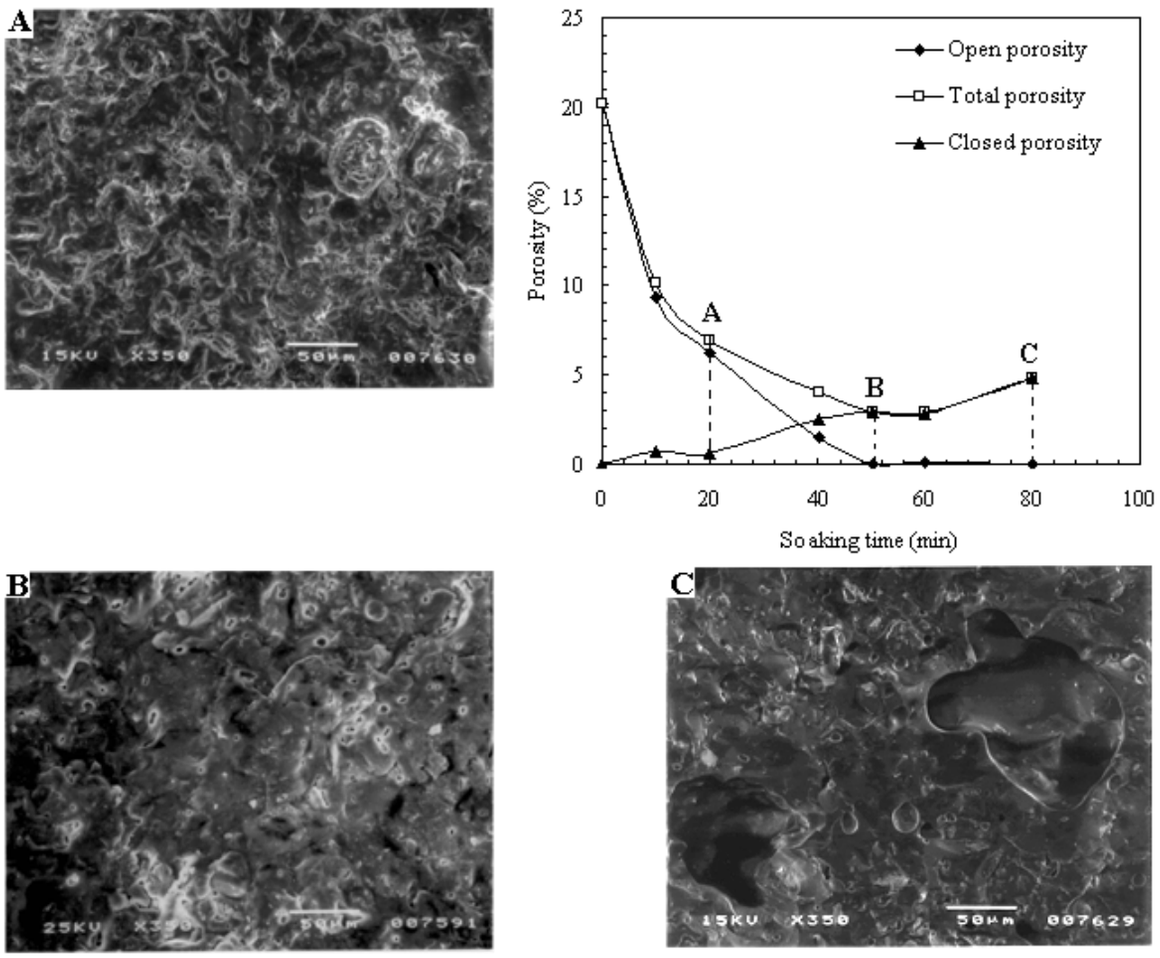

Figure 12. The variations of open, total and closed porosity as a function of soaking time for a typical porcelain stoneware composition.

In the sintering in the presence liquid phase two types of pressure act on the pores during the process. One of those is the capillary pressure, P_c, that is produced in the fine pores. The other one is the gas pressure inside the pores, P_g. The capillary pressure and gas pressure

http://dx.doi.org/10.5772/53259

work in opposite directions. Therefore, the total pressure, ΔP, is the difference between the two pressures, $\Delta P=P_c-P_g$. The general capillary pressure for spherical pores is given by equation 6 where r_1 is the average pore radius and γ is the surface free energy. In the first and intermediate stages of the sintering process the effect of gas pressure inside the pores on the sintering rate is assumed to be negligible as compared with the capillary pressure. In the final sintering stage, where the pores are almost closed, the pressure of the gas inside the pores becomes high and influences the sintering rate. The minimum porosity is where the gas pressure becomes equal to the capillary pressure. After this point, the total and closed porosity both increase and the pieces expand with increasing soaking time. Since the sintering process is finished when minimum porosity is reached, in this section the change in total porosity is investigated until this point. In developing the model for this phenomenon we considered an average radius, r_1, for a total of pores which are surrounded by a spherical shell and an equal amount of real incompressible material with radius of r_2 [24].

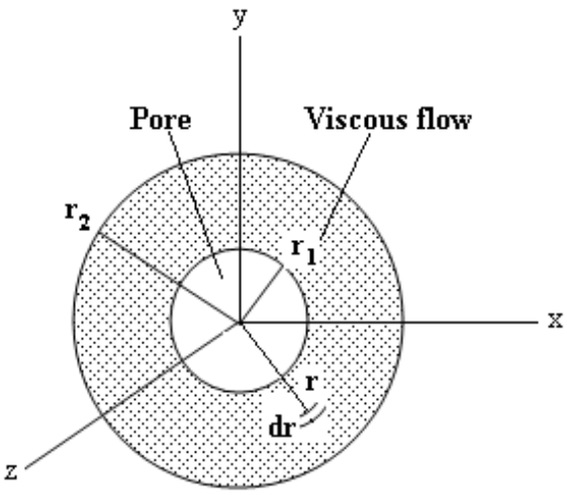

Figure 13. The diffusion of materials into spherical pore.

When an external or a negative internal pressure is applied, the flow of the material inside the shell decreases the pore volume by radial movement. Also, it is assumed that the variation in density of the liquid phase is negligible. Therefore, the porosity of the system, ε, is expressed as:

$$\varepsilon = \left(\frac{r_1}{r_2} \right)^3 \tag{12}$$

If we assume Newtonian behavior and creeping conditions for the system, the mass and momentum balance can be written in spherical coordinates according to equations 9 and 11:

Mass balance:

$$u_r r^2 = u_1 r_1^2 \tag{13}$$

Momentum balance:

$$-\frac{\partial P}{\partial r} + \eta \frac{1}{r^2} \frac{\partial}{\partial r}\left(r^2 \frac{\partial u_r}{\partial r} \right) = 0 \tag{14}$$

where u_r and u_1 are the velocity of real material at radiuses r and r_1, respectively. Substituting equation 13 into equation 14 and integrating between capillary and atmospheric pressures, we obtain the flow velocity at the boundary between the pore and real material, u_1, as a function of total porosity:

$$\int_{-\frac{2\gamma}{r_1}}^{0} dP = \int_{r_1}^{r_2} 2u_1 \eta r_1^2 \frac{dr}{r^4} \tag{15}$$

$$u_1 = -\frac{3\gamma}{\eta} \frac{1}{1-\varepsilon} \tag{16}$$

The equation 16 shows that the velocity of pore and material boundary decreases as sintering reach minimum total porosity.

8. Porosity variation in isothermal viscous flow sintering

In the sintering process the compact powder is usually held at constant temperature and the porosity is measured as a function of soaking time. The volume of real material approximately remains constant and the total number of pores does not change, if they are all equal in size but, the pores really are not equal in size. The small pores disappear more rapidly than the larger ones, so that the total number of pores decreases as soaking time increases [22]. Therefore, it is important to evaluate the number of pores per unit volume of real material, n, to find the relationship between the different parameters. In this case the relationship between pore radius and porosity is given by:

$$r_1 = \left(\frac{3}{4\pi} \right)^{\frac{1}{3}} \left(\frac{\varepsilon}{1-\varepsilon} \right)^{\frac{1}{3}} \left(\frac{1}{n} \right)^{\frac{1}{3}} \tag{17}$$

and, since $u_1 = dr_1/dt$, substituting equation 17 into equation 16 we find:

http://dx.doi.org/10.5772/53259

$$-\frac{d\varepsilon}{dt}=\left(\frac{9\gamma}{\eta}\right)n^{\frac{1}{3}}\left(\frac{4\pi}{3}\right)^{\frac{1}{3}}\varepsilon^{\frac{2}{3}}(1-\varepsilon)^{\frac{1}{3}} \tag{18}$$

The densification process of compact body is usually carried out at constant temperature in experimental scale and total porosity is measured as a function of soaking time. The obtained results by Orts et al. showed that the pores with small dimensions are eliminated during sintering process and the average pore size increases continuously [22]. Theoretically, it is assumed that total number of the pores per unit of real volume of material do not change if their dimensions are equal during sintering process. Also, the average volume is considered for all of the pores. If the equation 18 is integrated, it is possible to calculate the soaking time as a function of total porosity:

$$\int_{\varepsilon_0}^{\varepsilon}-\frac{d\varepsilon}{\varepsilon^{\frac{2}{3}}(1-\varepsilon)^{\frac{1}{3}}}=a\int_0^t dt \tag{19}$$

where $a=(9\gamma/\eta)n^{1/3}(4\pi/3)^{1/3}$. The left part of above equation can be easily evaluated by substituting $x^3 = \varepsilon/(1-\varepsilon)$ and the result is summarized as a follows:

$$F(x)-F(x_0)=at \tag{20}$$

$$F(x)=\frac{1}{2}\ln\frac{x^3+1}{(x+1)^3}-\sqrt{3}\tan^{-1}\left(\frac{2x-1}{\sqrt{3}}\right) \tag{21}$$

$F(x_0)$ is the value of F(x) if the sintering process is started at $\varepsilon = \varepsilon_0$. The effective viscosity of the system largely depends on the amount and viscosity of liquid phase formed from the quartz and fluxing agents present in the mix. Consequently, evaluation of the effective viscosity is very complex. According to Sack and Vora [25] the effective viscosity of a system non-linearly varies with time. Also, it was shown that the average pore size of compact body changes non-linearly in isothermal conditions [22]. The surface tension is assumed to be constant [15,16]. Therefore, the generalized form of equation 20, which is applicable for all the materials that are sintered in the presence of liquid phase, can be expressed by following equation:

$$F(x)-F(x_0)=at^b \tag{22}$$

The parameters of equation 22 can be obtained by non-linear regression method. The constant of a must be related to surface tension/viscosity ratio of system and total number of the pores per unit volume of real material.

The total porosity–soaking time plots shown in Figure 14 refer the sintering of a special porcelain stoneware composition at three firing temperatures. All curves are identical in nature and are characterized by exponential behavior. This kind of plot is generally observed in sintering in the presence of liquid phase. The observed exponential behavior can be attributed to diffusing liquid phase formed at high temperatures. The total porosity decreases as soaking time rises, expect for temperature and soaking times that body undergoes over firing followed by expansion of air inside the occluded pores. The decrease in total porosity is result of diffusing liquid phase into the open pores due to capillary pressure. As the sintering progresses, the closed pores grow and open pores are transformed into the closed pores. Finally, the total porosity increases due to expansion of air into the closed pores, leading to an expansion in body dimensions. It is obvious that there is a clear increase in densification rate with increase in temperature [24].

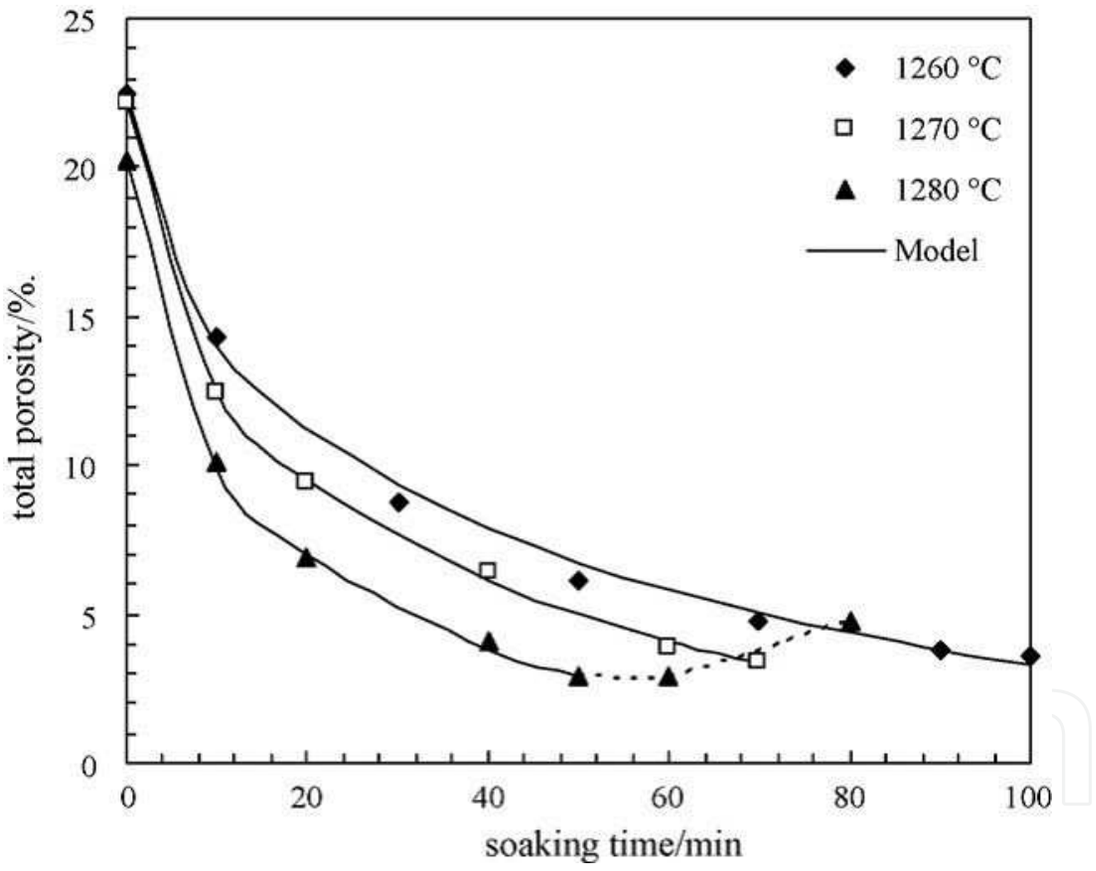

Figure 14. The variations of total porosity as a function of soaking time for a typical porcelain stoneware composition sintered at three different temperatures [26].

In order to obtain the parameters of equation 22 and thereby to calculate the total porosity for each body composition, the modified model is used to correlate total porosity-soaking time data. This equation is significantly complex model and depicts structural changes taking place in the pores of body during sintering process. Equation 22 also is used for estimating exponential behavior of total porosity-soaking time data. Since the sintering of body

http://dx.doi.org/10.5772/53259

occurs by diffusing liquid phase and takes place by capillary forces, application of this model is justified. Model parameter, a, is related to kinetic rate constant and depends on temperature. Parameter b is related to physical changes occurring in ceramic body matrix. This parameter is very important since its value determines the total porosity characteristics. Thus for b=1, the total porosity changes follows homogenous first order kinetic. For b<1 a exponential behavior is guaranteed. The model given by equation 22 is a general one and is applicable to all temperatures and compositions. A non-linear plot of $F(x)-F(x_0)$ versus t will give the values of a and b [26]. The total porosity–soaking time data fit the model very nicely. From the parameters of the non-linear correlations, the constants of a and b are easily calculated. By use of the constant parameters the rate constant is computed in each temperature. For example, the values of a and b are tabulated in Table 2 for a typical porcelain stoneware body and compositions containing different amounts of nepheline syenite. The value of b virtually remains constant for each composition whilst the parameter a increases considerably as sintering temperature rises.

9. Kinetics of viscous flow sintering

If the values of a are plotted versus the inverse of temperature on semi-logarithm scale according to equation 23, the plots fit straight lines well, which indicate that the variation of a, with temperature may be represented by an exponential equation form as a follows:

$$a = a_0 \exp\left(-\frac{Q}{T}\right) \tag{23}$$

where a_0 and Q are the constant parameters. Table 3 details the values of these parameters. Since sintering process takes place in the presence of liquid phase, the rate of densification defined in term of rate constant, k(ε), varies continuously with soaking time due to continuous structural changes in pores of ceramic body. The densification rate can be expressed as following equation:

$$-\frac{d\varepsilon}{dt} = k(\varepsilon) \tag{24}$$

The expression for the rate constant is given by following equation:

$$k(\varepsilon) = b a^{\frac{1}{b}} \frac{\left[F\left(\sqrt[3]{\frac{\varepsilon}{1-\varepsilon}}\right) - F\left(\sqrt[3]{\frac{\varepsilon_0}{1-\varepsilon_0}}\right)\right]^{\frac{b-1}{b}}}{\sqrt[3]{\frac{\varepsilon}{1-\varepsilon}}} \tag{25}$$

k(ε) can be calculated at each total porosity, for example in minimum total porosity. Arrhenius plots can be applied for different compositions according the following equation:

$$k(\varepsilon)=k_0\exp\left(-\frac{E_a}{RT}\right) \tag{26}$$

Nepheline syenite (wt. %)	Temperature (ºC)	a	b
0.0	1260	0.0897	0.5035
	1270	0.1073	0.4940
	1280	0.1231	0.4973
5.0	1240	0.0435	0.7043
	1250	0.0578	0.7089
	1260	0.0702	0.7134
10.0	1240	0.0357	0.8182
	1250	0.0480	0.8196
	1260	0.0593	0.8127
15.5	1240	0.0235	0.9438
	1250	0.0306	0.9587
	1260	0.0442	0.9205

Table 2. The constant values of equation 22 for a typical and modified porcelain stoneware compositions [26].

Nepheline syenite (wt. %)	a_0	Q (K)
0.0	4.3×10^{9}	37689
5.0	2.2×10^{14}	54719
10.0	2.9×10^{15}	58871
15.5	2.4×10^{19}	73235

Table 3. The parameters of equation 26 for a typical and modified porcelain stoneware compositions [26].

where E_a is activation energy, k_0 is the frequency factor and R is the constant of ideal gas. The values of kinetic parameters are presented in Table 4. Also, the values of activation energy special compositions are shown in Figure 15 at three values of total porosity as a function of nepheline syenite content. This range of porosity is considered because it covers all of the minimum porosity values for special compositions. The value of activation energy approximately remains constant for each composition in the domain of porosity. The value of this parameter increases, reaching to maximum value in the presence 5.0 wt.% of nepheline

syenite. This phenomenon indicates that the mechanism of pore changes in ceramic structure is different in the presence mentioned amounts of nepheline syenite.

The total porosity changes involve typically with surface tension/viscosity ratio of liquid phase that increases as nepheline content reaches to 5.0 wt.% in body composition. As the amount of nepheline syenite rises in body composition this ratio falls down because of dissolving quartz and mullite crystals in melted phase [11]. The surface tension/viscosity ratio of liquid phase grows and reaches maximum value in the presence of 5.0 wt.% nepheline syenite, Figure 16 [16]. The increase in surface tension/viscosity ratio accelerates the removal rate of porosity but the more increase in nepheline content cannot positively increase the surface tension/viscosity ratio. Therefore, the increment of nepheline syenite content in body composition has negligible role on densification rate of body. The trends of these changes in kinetic parameters show an overall positive effect on densification rate and as a result, total porosity decreases considerably in the presence 5.0 wt.% nepheline syenite. The addition of nepheline syenite in porcelain stoneware composition results an increase in activation energy and frequency factor for composition prepared with 5 wt.% nepheline syenite. Finally, the variations of kinetic parameters improve the densification rate in the presence of 5.0 wt.% nepheline syenite. The densification of a porcelain stoneware body is governed by the viscosity of the liquid phase formed at high temperature which is controlled by the Na_2O+K_2O content. The Na_2O/K_2O ratio is also a controllable factor on viscosity of liquid glassy phase. In the compositions modified by nepheline syenite, the bodies contain more Na_2O with lower amount of K_2O and SiO_2. Although, potassium oxide leads to a liquid phase with less viscosity compared to sodium oxide but, increasing Na_2O+K_2O content and low content of silica in modified compositions are compensated this negative effect. These variations bring about a lower viscosity of liquid phase in materials containing nepheline syenite. Fluxing agent like nepheline syenite should help in enhancing the densification rate of ceramic bodies if melted phase viscosity is reduced by addition fluxing agent. The rate constant is improved in the presence 5.0 wt.% nepheline syenite. The addition of nepheline syenite content more than 5.0 wt.% has negligible role in densification rate. Therefore, the viscous melted phase is not able to diffuse into the pores by capillary pressure since viscosity of liquid phase is not effectively influenced by nepheline syenite content especially at low sintering temperature.

Nepheline syenite (wt. %)	k_0 (min^{-1})	E_a (kJ/mol)
0.0	7.4×10^{19}	76.7
5.0	8.8×10^{24}	92.3
10.0	1.8×10^{19}	71.7
15.5	9.6×10^{17}	66.9

Table 4. The kinetic parameters of Arrhenius equation for a typical and modified porcelain stoneware compositions [26].

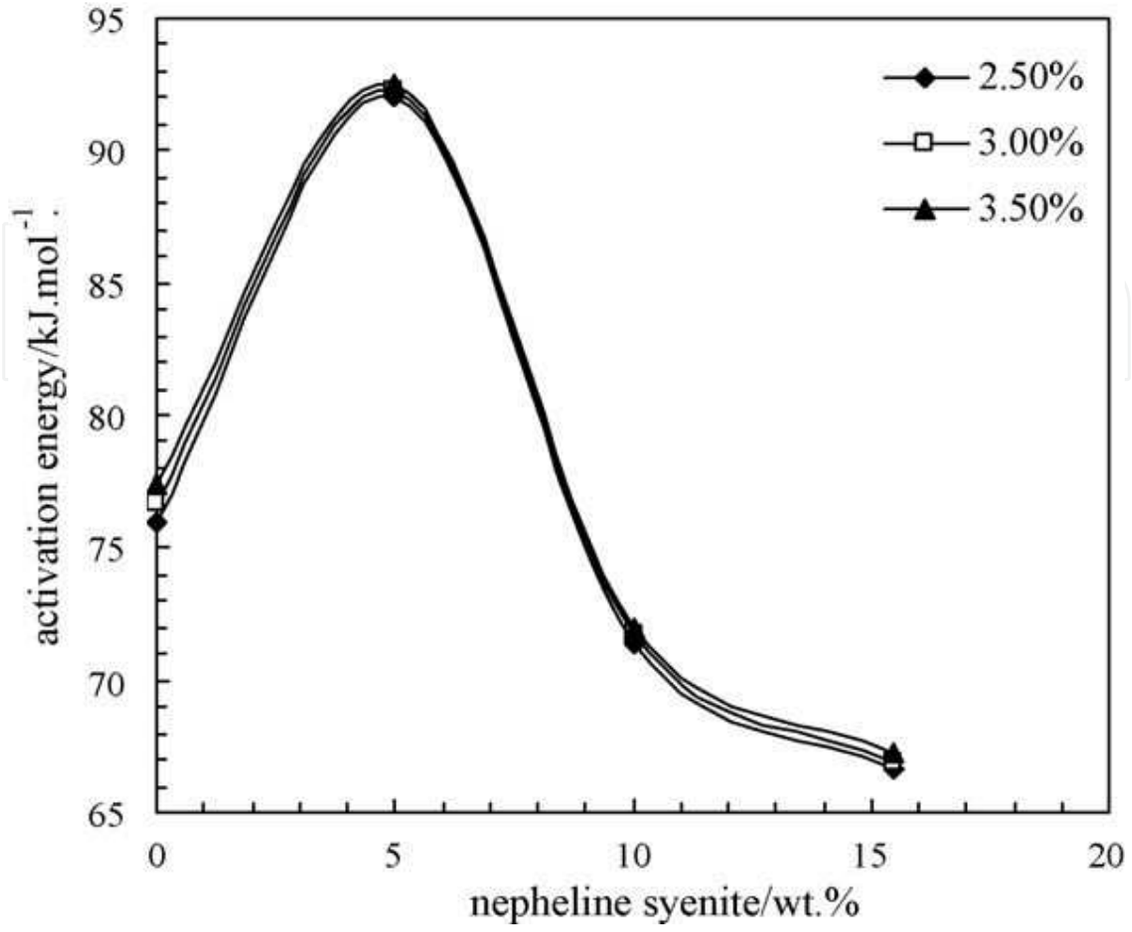

Figure 15. The variation of activation energy as a function of nepheline syenite content at three different total porosity [26].

10. Role of particle size distribution on sintering

As previously discussed in section 4, the particle size distribution of composition can effectively influence sintering process. For example - if the composition containing 10 wt.% nepheline syenite milled during 8 and 12 h is considered, Figure 11, the kinetic parameters of equations 23 and 26 are summarized in Tables 5 and 6, respectively. The values of activation energy this composition show that the increase in milling time changes the activation energy values considerably, indicating that the mechanism of sintering in these particular cases are different due to changes in surface tension/viscosity ratio. An increase in the specific surface area of particles is sufficient to increase the sintering rate. The particle size distribution of raw materials is more important factor in densification rate and plays a beneficial role on specific surface area of materials to absorb energy. This is evident from the fact that the value of frequency factor which is the function of specific surface area is more in the composition milled for 12 h. The increase in milling time ensures a higher surface area to improve the densification rate.

http://dx.doi.org/10.5772/53259

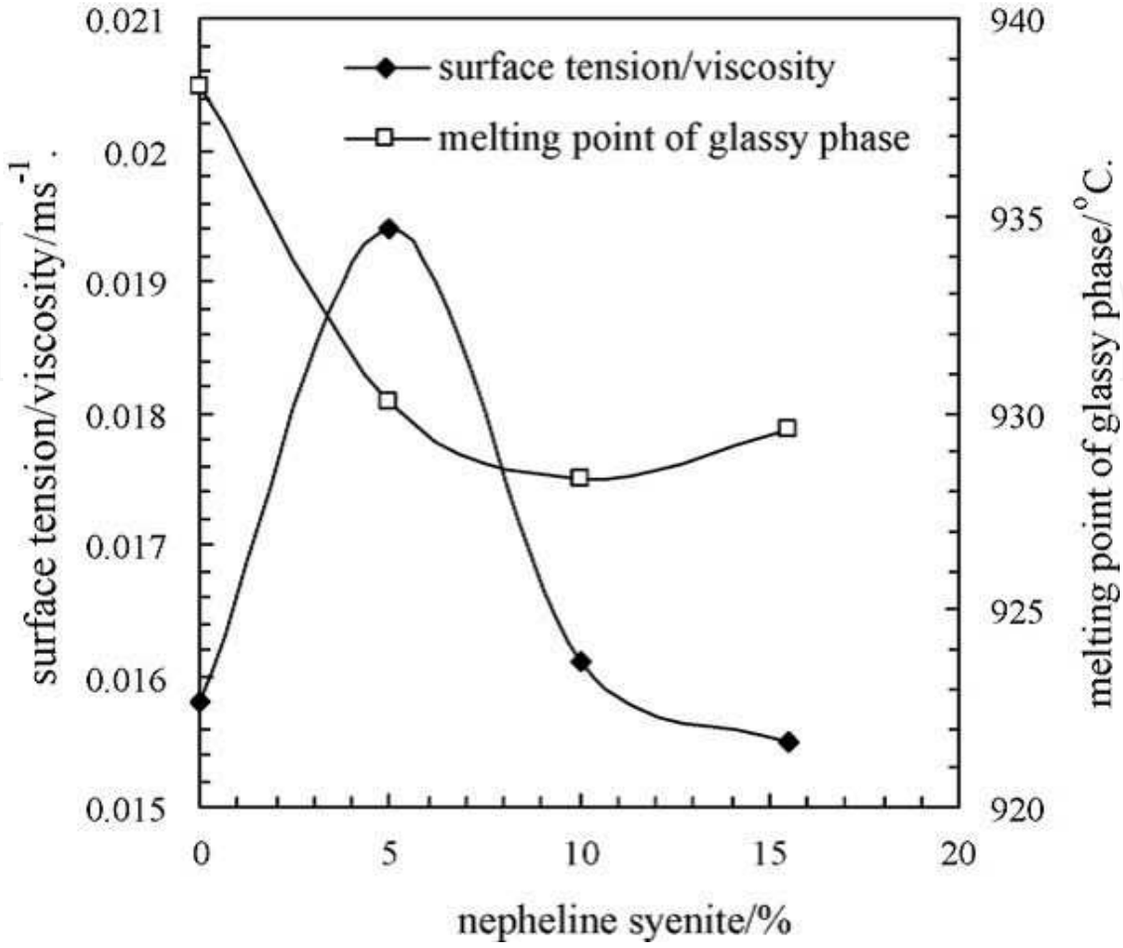

Figure 16. The variations of surface tension/viscosity ratio of liquid phase and melting point of glassy phase of porcelain stoneware body with nepheline syenite content [16].

Milling time (h)	a_0	Q (K)
8	2.9×10^{15}	58871
12	7.0×10^{17}	66623

Table 5. The parameters of equation 23 for a porcelain stoneware composition containing 10 wt.% nepheline syenite milled at different time [26].

Milling time (h)	k_0 (min^{-1})	E_a (kJ/mol)
8	1.8×10^{19}	71.7
12	1.2×10^{25}	91.9

Table 6. The kinetic parameters of Arrhenius equation for a porcelain stoneware composition containing 10 wt.% nepheline syenite milled at different time [26].

After substation equation 23 into equation 22, the following equation is developed to relate the optimum soaking time to temperature:

$$\ln t_{opt} = A + \frac{B}{T} \tag{27}$$

where t_{opt} is the optimum soaking time to achieve minimum value of total porosity and A, B are the model constants that are reported in Table 7 for mentioned compositions. The validity of this model for obtaining optimum soaking time in other temperatures for a typical porcelain stoneware composition is summarized in Table 8. The agreement between experimental data and model predictions is again excellent [26].

Nepheline syenite (wt. %)	Milling time (h)	A (h)	B(K^{-1})
0.0	8	-4444.6	697.7
5.0	8	-2858.8	442.6
10.0	8	-1198.0	187.7
15.5	8	-1923.1	297.9
10.0	12	-1912.6	295.6

Table 7. The parameters of equation 27 for a typical and modified porcelain stoneware compositions [26].

Soaking time (min)	1230 ºC		1240 ºC		1250 ºC	
	$\varepsilon_{exp.}$ (%)	$\varepsilon_{cal.}$ (%)	$\varepsilon_{exp.}$ (%)	$\varepsilon_{cal.}$ (%)	$\varepsilon_{exp.}$ (%)	$\varepsilon_{cal.}$ (%)
120					3.51	3.64
180			3.22	3.51		
260	3.51	3.88				

Table 8. Experimental and calculated values of total porosity for a typical porcelain stoneware composition corresponding to minimum value of 3.51 % [26].

11. Conclusions

Because of the complex interplay between the ceramic materials and the kinetics of sintering, the viscous flow represents some of most complicated systems. Due to importance of liquid phase motion, momentum balance is required to develop fundamental equation for understanding sintering. Major challenges are the development of kinetic model and improvement of viscous flow sintering theory. The liquid phase diffusion may produce unsatisfied microstructure. The sintering behavior of ceramic materials is affected by surface tension/viscosity

ratio. The surface tension is not altered by material composition in silicate systems such as porcelain and porcelain stoneware bodies. Surface wetting of liquid phase produces capillary phenomena in porous ceramic systems. In this chapter a complicated model was presented for studying viscous flow sintering. For achieve an acceptable firing profile the relation between soaking time and temperature should be determined. Since the surface tension/viscosity ratio controls total porosity during the sintering, increasing fluxing oxides enhances the removal rate of total porosity. A modified kinetic model was proposed to describe the variation of total porosity during the isothermal sintering with temperature and soaking time. Also, the value of frequency factor which is function of specific surface area, increases as the composition is prepared at high milling time. The proposed model can be used for the bodies that are sintered in the presence of melted phase to achieve minimum porosity at each temperature. It is possible to estimate the proper soaking time to obtain minimum total porosity at a given firing temperature. The data of theoretical porosity are very similar to the experimental one. In summary, the alkali oxides accelerate the sintering process by reducing viscosity of liquid phase. In effect at constant temperature the soaking time is reduced by increasing temperature.

Nomenclature

constant parameter (s)	A
particle area (m^2)	A_p
constant parameter	a
constant parameter	a_0
constant parameter (K)	B
constant parameter	b
activation energy (kJ/mol)	E_a
porosity function	$F(x)$
value of F(x) for $\varepsilon = \varepsilon_0$	$F(x_0)$
external force per unit volume (N/m^3)	f_g
Gibb's free energy (kJ/mol)	G
rate constant (s^{-1})	$k(\varepsilon)$
frequency factor (s^{-1})	k_0
characteristic length (m)	l
number of species	N_i
Reynolds number	N_{Re}
number of pores per unit volume of real material	n
pressure (Pa)	P
capillary pressure (Pa)	P_c
gas pressure (Pa)	P_g
pressure difference (Pa)	ΔP
constant parameter (K)	Q
constant of ideal gas (kJ/mol. K)	R
average radius of pore (m)	r_1
average radius of material (m)	r_2

temperature (K)	T
time (s)	t
optimum soaking time (s)	t_{opt}
velocity (m/s)	u
velocity of real material at radius of r_1 (m/s)	u_1
velocity of real material at radius of r (m/s)	u_r
volume difference (m^3)	ΔV
porosity variable	x
quartz allotrope	α
quartz allotrope	β
surface tension (N/m)	γ
total porosity	ε
initial porosity	ε_0
fluid viscosity (Pa. s)	η
fluid density (kg/m^3)	ρ
shear stress (Pa)	τ

Acknowledgements

Many peoples have made valuable information in ceramic center of Bologna, Italy. We wish to express our thanks to: Prof. G. Timellini, Dr. E. Rastelli, Dr. A. Tucci, Dr. L. Esposito, Dr. A. Albertazzi, Mr. S., Degli Esposti and Mr. D. Naldi.

Author details

Shiva Salem[1] and Amin Salem[2,3*]

*Address all correspondence to: a_salem@iust.ac.ir

1 Chemical Engineering Group, Orumiyeh Industrial University, Orumiyeh, Iran

2 Center of Excellence for Color Science and Technology, Tehran, Iran

3 Chemical Engineering Department, Sahand University of Technology, Tabriz, Iran

References

[1] Reed JS. Introduction to Principles of Ceramic Processing. 2nd ed., John Wiley and Sons, New York, USA; 1995.

[2] Funk JE. Designing the Optimum Firing Curve for Porcelains. Ceramic Bulletin 1982; 62(6) 632-635.

[3] Mackenzie RC. Differential Thermal Analysis. 2nd ed., Academic Press, London, UK; 1973.

[4] Mclaughlin RJW. Differential Thermal Analysis of Kaolinite – Illite Mixtures. British Ceramic Transactions1960; 59 178-187.

[5] Aldo R. Boccaccini AR., Trusty PA. In Situ Characterization of the Shrinkage Behavior of Ceramic Powder Compacts during Sintering by Using Heating Microscopy. Materials Characterization 1998; 41 109-121.

[6] Ahmed M., Earl DA. Characterizing Glaze Melting Behaviour via HSM. American Ceramic Society Bulletin 2002; 81(3) 47-51.

[7] Salem, Sh., Jazayeri SH., Bondioli F., Allahverdi A., Shirvani, M. Characterizing Thermal Behaviour of Ceramic Glaze Containing Nano-Sized Cobalt-Aluminate Pigment by Hot Stage Microscopy. Thermochimica Acta 2011; 521(1-2) 191-196.

[8] Salem A., Jazayeri SH., Rastelli E., Timellini G. Dilatometeric Study of Shrinkage during Sintering Process for Porcelain Stoneware Body in Presence of Nepheline syenite. Journal of Materials Processing Technology 2009; 209 1240-1246.

[9] Carty WM., Senapati U. Porcelain Raw Materials, Processing, Phase Evolution and Mechanical Behavior. Journal of American Ceramic Society 1998; 81(1) 3–20.

[10] Lee WE., Iqbal Y. Influence of Mixing on Mullite Formation in Porcelain. Journal of European Ceramic Society 2001; 21 2583-2586.

[11] Esposito L., Salem A., Tucci A., Gualtieri A., Jazayeri SH. The Use of Nepheline-Syenite in a Body Mix for Porcelain Stoneware Tiles. Ceramics International 2005; 31 233–240.

[12] Klein G. Application of Feldspar Raw Materials in the Silicate Ceramics Industry. Interceram 2001; 50 (1–2) 8–11.

[13] Rogers WZ. Feldspar and Nepheline Syenite. Ceramic Engineering Science Proceeding. 2003; 24 272–283.

[14] Kingery WD., Bowen HK., Uhlmann DR. Introduction to Ceramics. Wiley-Interscience, New York, USA; 1976.

[15] Matteucci F., Dondi M., Guarini G. Effect of Soda – Lime Glass on Sintering and Technological Properties of Porcelain Stoneware Tiles. Ceramics International 2002; 28 873-880.

[16] Salem A., Jazayeri SH., E. Rastelli E., Timellini G. Effect of Nepheline Syenite on the Colorant Behavior of Porcelain Stoneware Body. Journal of Ceramic Processing Research 2009; 10(5) 621-627.

[17] Slattery JC. Advanced Transport Phenomena. Cambridge University Press, Cambridge, UK; 1999.

[18] Bird RB., Stewart WE., Lightfoot EN. Transport Phenomena. 2nd ed., John Wiley and Sons, New York, USA; 2002.

[19] Barsoum WM. Fundamentals of Ceramics. McGraw Hill, New York, USA; 1996.

[20] Somiya S., Moriyoshi Y. Sintering Key Papers. Elsevier Applied Science, London, UK; 1990.

[21] Orts MJ., Amoros JL., Escardino A., Gozalbo A., Feliu C. Kinetic Model for Isothermal Sintering of Low Porosity Floor Tiles. Applied Clay Science 1993; 8 231-245.

[22] Orts MJ., Escardino A., Amoros JL., Negre F. Microstructural Changes during the Firing of Stoneware Floor Tiles. Applied Clay Science 1993; 8 193-205.

[23] Ducamp VC., Raj R. Shear and Densification of Glass Powder Compacts. Journal of American Ceramic Socity 1989; 72 798-804.

[24] Jazayeri SH., Salem A., Timellini G., E. Rastelli E. A Kinetic Study on the Development of Porosity in Porcelain Stoneware Tile Sintering. Boletin de la Sociedad Espanola de Cerámica y Vidrio 2007; 46(1) 1-6.

[25] Sacks MD., Vora SD. Preparation of SiO2 Glass from Model Powder Compact. Part III: Enhanced Densification by Sol Infiltration. Journal of American Ceramic Society 1988; 71, 245-249.

[26] Salem A., Jazayeri SH., E. Rastelli E., Timellini G. Kinetic Model for Isothermal Sintering of Porcelain Stoneware Body in Presence of Nepheline Syenite. Thermochimica Acta 2010; 503–504 1-7.